

See discussions, stats, and author profiles for this publication at: <https://www.researchgate.net/publication/231667570>

# Solvent-Dependent Stability of Monolayer-Protected Au<sub>38</sub> Clusters

ARTICLE *in* JOURNAL OF PHYSICAL CHEMISTRY LETTERS · NOVEMBER 2009

Impact Factor: 7.46 · DOI: 10.1021/jz900035p

---

CITATIONS

30

---

READS

22

6 AUTHORS, INCLUDING:



Outi Toikkanen

Aalto University

9 PUBLICATIONS 212 CITATIONS

SEE PROFILE



Amala Dass

University of Mississippi

108 PUBLICATIONS 3,196 CITATIONS

SEE PROFILE

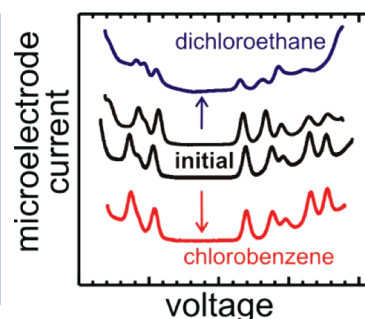
# Solvent-Dependent Stability of Monolayer-Protected Au38 Clusters

Outi Toikkanen,<sup>†</sup> Sanna Carlsson,<sup>†</sup> Amala Dass,<sup>§</sup> Gunilla Rönnholm,<sup>‡</sup> Nisse Kalkkinen,<sup>‡</sup> and Bernadette M. Quinn<sup>\*,†</sup>

<sup>†</sup>Department of Chemistry, Helsinki University of Technology, P.O. Box 6100, FIN-02015 HUT, Finland, <sup>§</sup>Department of Chemistry, University of Mississippi, University, Mississippi 3867, and <sup>‡</sup>Institute of Biotechnology, University of Helsinki, P.O. Box 65, FIN-00014 University of Helsinki, Finland

**ABSTRACT** Using a combination of electroanalytical techniques and mass spectrometry, we demonstrate that the stability of hexanethiolate-protected Au38 clusters is critically dependent on the dispersing solvent. In addition, the dispersing solvent significantly influences the cluster stability both in the presence of excess thiol and when charge is stored in the cluster core. The influence of the solvent should not be overlooked in synthesis and handling of monolayer-protected clusters.

**SECTION** Nanoparticles and Nanostructures



The origin of the magic core atom number for gold nanoparticles protected by a thiolate monolayer, the so-called monolayer-protected gold clusters (MPCs), has been the focus of intense theoretical and experimental interest.<sup>1–9</sup> The breakthrough in this area was the crystal structure determination for Au102 and later Au25.<sup>3,10,11</sup> These reports revealed that the monolayer is not composed of simple thiolates but rather Au thiolate oligomers that form a shell around the Au core, in a “divide and protect” motif initially proposed by Häkkinen and co-workers based on density functional theory calculations.<sup>4,12</sup> Experimentally, magic core numbers have been identified simply by their ability to resist etching in excess thiol solutions.<sup>7–9,13–20</sup> However, in this letter, we demonstrate that the resistance to etching as well as the charge-dependent stability can be dictated by the dispersing solvent rather than the inherent/intrinsic stability of the cluster.

Using a combination of electroanalytical techniques and mass spectrometry, we show that hexanethiolate-protected Au38 clusters are stable indefinitely in chlorobenzene (CB) but degrade over a matter of weeks in 1,2-dichloroethane (DCE). We report that solvent-assisted monolayer desorption is the underlying reason for the irreversible aggregation of the clusters. Mass spectra reveal that the desorbing species are gold thiolates, consistent with the structure motif of a Au core surrounded by ring-like Au thiolate oligomers.<sup>4,11</sup> Using a novel generation–collection electroanalytical technique, we demonstrate experimentally that the stability of the monolayer as a function of the charge stored in the core is strongly solvent-dependent. Moreover, we report that the stability of the clusters in excess thiol solution is unexpected. Au38 clusters are indefinitely stable in DCE solutions containing a hyperexcess of thiol, while larger clusters are etched. However, when the solvent is changed to CB, there is no evidence that Au38 has special stability in excess thiol relative to other core sizes.

**Solvent-Dependent Stability of Charge Neutral Au38 Clusters:** Au38 was dispersed in DCE and CB at approximately identical concentrations and kept in solution under ambient conditions. Microelectrode square wave voltammograms (SWVs) were recorded at given intervals over a period of time. Representative examples are given in Figure 1. The SWVs obtained for clusters dispersed in CB did not evolve over time, with the voltammograms recorded on day 1 and day 55 being practically identical. In contrast, for clusters dispersed in DCE, the charging pattern began to evolve and after 66 days had no features that could be ascribed to the presence of Au38. There was also evidence of precipitation. The precipitate did not redisperse, indicating that irreversible aggregation of the cores had occurred. After 66 days, the “impurity” peaks at 1 and –1.2 V marked with an asterisk in Figure 1c are the only peaks that are apparent in the SWV. These impurity peaks have usually been ascribed to the residual polydispersity, where clusters with smaller cores and thus larger HOMO–LUMO gaps are present in solution.<sup>21,22</sup>

The electrified liquid–liquid interface was used to probe the ionic species present in solution.<sup>23,24</sup> A micropipet containing the aqueous phase (10 mM LiCl) was immersed in the organic phase solution containing Au38 and cyclic voltammograms (CVs) recorded at the water/organic interface formed at the micropipet tip over the same time period as that for the microelectrode studies.

For the clusters dispersed in CB, the CVs recorded at the w/CB interface in the presence and absence of Au38 are identical and do not vary over a 55 day period. In contrast, a positive current offset becomes apparent over time in the corresponding CVs recorded at the w/DCE interface in the presence of

**Received Date:** September 23, 2009

**Accepted Date:** October 26, 2009

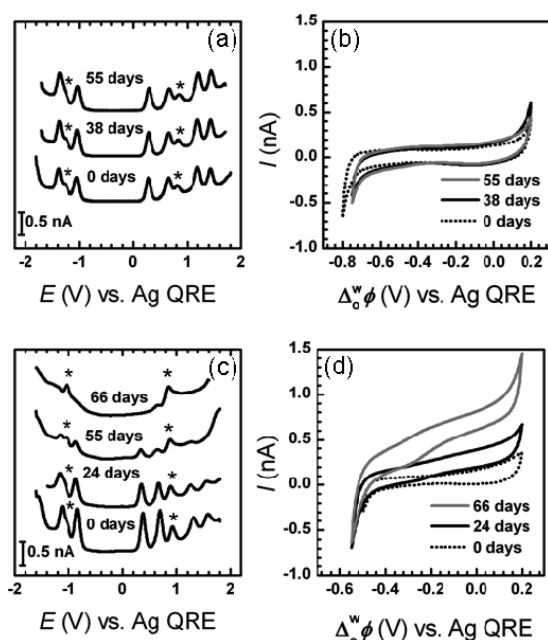


**Figure 1.** Microelectrode SWVs for Au38 dispersed in CB (a) and DCE (c) recorded over a period of time and the corresponding CVs recorded at the w/CB (b) and w/DCE (d) interfaces supported at the tip of a micropipet. The impurity peaks are marked with asterisks.

Au38, and this offset increased over time. Due to the diffusion regime to the micropipet-supported interface, the current can only be due to an anionic species transferring from the organic to the aqueous phase.<sup>24,25</sup> As there is current offset throughout the available interfacial potential ( $\Delta\phi^w$ ) window, this indicates that the anion is relatively hydrophilic, preferring to be in the aqueous phase for all applied values of  $\Delta\phi^w$ .<sup>23–25</sup> The current offset increases gradually over a period of weeks, indicating that the bulk concentration of anions in the DCE phase is increasing. As can be seen from Figure 1, the evolutions in the microelectrode SWV and the micropipet CV are correlated. In the case of CB, there is no evolution in the microelectrode charging pattern and no offset in the micropipet CV, while for DCE, the gradual disappearance of the Au38 charging peaks in the microelectrode SWVs occurs concurrently with the increase in the current offset in the w/DCE micropipet CVs.

To determine the nature of the species present in the Au38 DCE solution after 55 days, LDI mass spectrometry was used (see Figure 2). The LDI mass spectrum shows that the only species present in solution are short Au thiolate oligomers. A mass peak ascribable to Au38 is absent, as are peaks in the 2–3 kDa range that would indicate the presence of Au11–Au13 species. Thus, it is clear that the impurity voltammetric peaks in the SWVs given in Figure 1 are not due to the presence of smaller clusters, as previously postulated.<sup>21,22</sup> As there are no larger clusters that can be fragmented, the peaks in the 0–1 kDa region are due to species present in solution. However, it is not possible to conclusively determine the exact composition of the desorbing species as not all peaks can be identified. The identifiable masses correspond to species with one Au atom ( $\text{AuS}_2$ ,  $\text{AuSR}$ ,  $\text{AuS(SR)}$ ,  $\text{Au(SR)}_2$ ), two Au atoms ( $\text{Au}_2\text{S(SR)}_2$  and  $\text{Au}_2(\text{SR})_3$ ), or even three Au

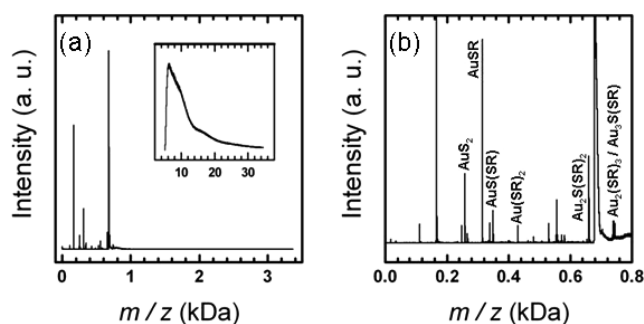


**Figure 2.** LDI-TOF mass spectrum of a solution of Au38 dispersed in DCE after 55 days in solution. (a) Negative ion mode in the range of Au thiolate oligomers and Au11–Au13 clusters. The inset shows the range where Au38 and larger clusters would be detected (positive ion mode). (b) Magnification in the low mass range, showing peaks corresponding to Au thiolate oligomers.

atoms ( $\text{Au}_3\text{S(SR)}$ ). AuSR oligomers larger than three gold atoms in the Au–S chain can be excluded. The other peaks are likely to be oligomer fragments and new species formed due to the harsh ionization conditions employed.<sup>26</sup> As the proposed structure of Au38 involves a gold core protected by ring-like  $\text{Au(SR)}_2$  and  $\text{Au}_2(\text{SR})_3$  units,<sup>5</sup> the species detected can be ascribed to the protecting monolayer, that is, the monolayer has desorbed from the core as Au thiolates rather than simple thiolates. In contrast, the mass spectrum for Au38 recorded immediately after preparing the DCE solution showed a broad peak typical for Au38 and extensive fragmentation peaks apparent in the 0–1 kDa region (Supporting Information). None of the spectra obtained had mass peaks in the 2–3 kDa range that could be ascribed to the presence of Au11 and Au13.

Correlating the mass spectrometry data with the microelectrode and micropipet voltammograms, it can be concluded that the impurity peaks in the SWVs are due to Au thiolate oligomers. These species were not detected at the w/DCE or w/CB interfaces, implying that they are either uncharged or relatively hydrophobic.<sup>23–25</sup> The species detected at the micropipet w/DCE interface is a Au thiolate species that is both anionic and hydrophilic.<sup>23–25</sup>

From the microelectrode, micropipet, and mass spectrometry studies, it is apparent that the stability of Au38 clusters in solution is strongly solvent-dependent, with the clusters being stable indefinitely in CB and unstable in DCE. After 55 days in DCE solution, the clusters are completely degraded. The metal cores aggregate and precipitate out of solution, leaving the Au thiolates from the monolayer in solution.

**Solvent-Dependent Stability of Charged Au38 Clusters:** As MPC monolayer desorption is known to be dependent on the charge stored in the core (akin to the reductive desorption of a conventional SAM formed on a macroscopic Au electrode),<sup>21,24,27</sup> we next used an electroanalytical generation–collection method to investigate the influence of the solvent on the charge-dependent desorption.<sup>23,24</sup> The measurements involved voltammetry at a Pt-coated micropipet-supported water–organic interface. The measurement principle is analogous to the conventional ring–disk electrode used in electroanalysis and is illustrated schematically in

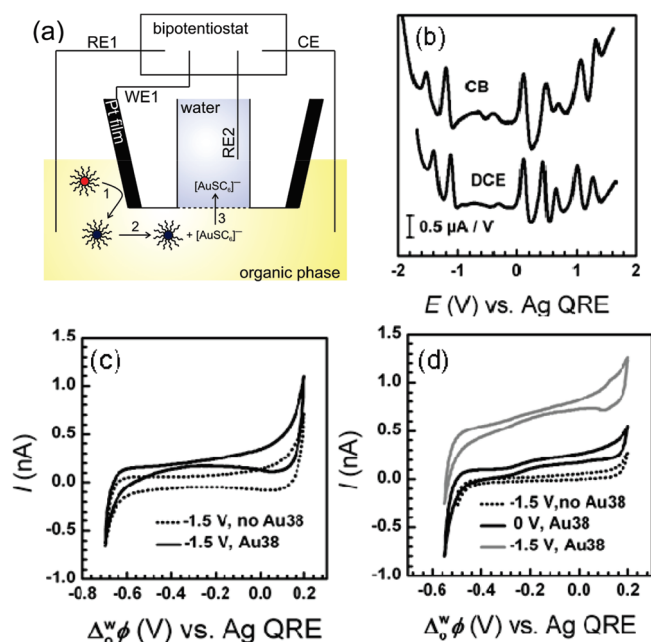


**Figure 3.** (a) Schematic of the electroanalytical generation–collection method utilizing the Pt coat electrode as the generator electrode and the micropipet-supported water–organic interface as the ion detector interface; (b) derivatives of CVs recorded at the generator electrode in the presence of Au38 clusters dispersed in DCE and CB; CVs recorded at the detector w/DCE (c) and w/CB (d) interfaces in the presence of Au38 in the organic phase with the generator electrode biased at  $-1.5$  and  $0$  V (generating the  $\text{Au38}^{2-}$  and  $\text{Au38}^0$  states, respectively). The dotted lines in both plots show the control CVs obtained in the absence of Au38 with the generator electrode biased at  $-1.5$  V. For the w/CB interface, the CV obtained in the presence of Au38 with the generator biased at  $0$  V was identical to that recorded in the absence of Au38 (control CV dotted line in (c)).

Figure 3a. Here, the Pt outer coat of the micropipet functions as the generator electrode, and Au38 can be locally charged to a given charge state,  $z$ , through control of the coat electrode potential (process 1 in the schematic).<sup>23,24</sup> This results in a high concentration of charged clusters in the vicinity of the micropipet-supported water–organic interface (process 2 in the schematic). Ionic species desorbed from the charged cluster can be detected at this ion detector interface (process 3 in the schematic).<sup>23,24</sup> It is important to reiterate that the charged clusters themselves do not transfer, and any increase in current can be ascribed to the transfer of ionic species desorbed from the charged cluster surface. Derivatives of CVs recorded at the Pt coat electrode for Au38 dispersed in DCE and CB are given in Figure 3b. The charging patterns are consistent with those obtained at the Pt microelectrode solution interface (Figure 1a and c), indicating that the coat electrode is functioning well and that the IR drop is not significant, despite its macro dimensions. The CV response of the detector interface in the absence of Au38 is the baseline response and is given by dotted lines in Figure 3c and d. In the presence of Au38, there is no change in the CV response when the particles are dispersed in CB (not shown) and a slight current offset when they are dispersed in DCE. In the generation–collection mode, biasing the generator electrode to a

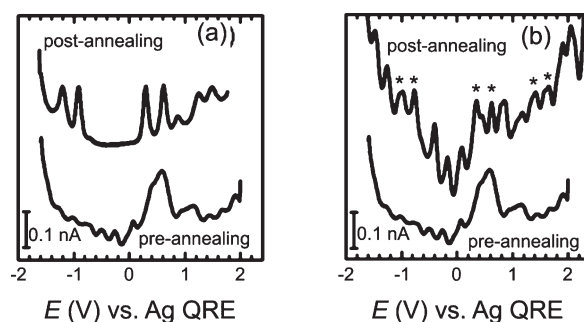


**Figure 4.** Microelectrode SWVs for particles postannealing (upper traces) in either (a) DCE or (b) CB compared with the response preannealing (lower trace in both plots). All SWVs were recorded in DCE solution containing  $10$  mM base electrolyte. In (b), the peaks ascribable to Au38 are marked with asterisks.

potential ( $-1.5$  V versus QRE) to generate the  $-2$  cluster charge state results in very different CV responses at the detector interface depending on the solvent used. In the case of CB, there is a slight positive offset from the zero current line in the micropipet response (Figure 3c), while for DCE, the current offset is marked (Figure 3d). In both cases, the current offset is due to anions transferring from the organic to the aqueous phase, and in both cases, the CV response also returned to the zero current baseline value when the generator electrode was biased at less reducing potential ( $z = 0$ ). The anions detected are thiolate species desorbed from the clusters after they are reduced at the generator electrode. This anion transfer at the detector interface was only apparent when the  $-1$  (data not shown) and  $-2$  cluster charge states were generated at the Pt coat electrode. The current offset increased with the Au38 charge number, indicating that more anions were available to transfer as the cluster charge number was increased from  $-1$  to  $-2$ . Control experiments in the absence of Au38 in DCE did not induce current offset in the detector CV response. As the reduced clusters  $\text{Au38}^{1-}$  and  $\text{Au38}^{2-}$  do not transfer, anions desorbing from the reduced clusters are the only possible source for the detector current response. The desorption of thiolate species from the reduced Au38 cluster is not unexpected based on the literature.<sup>21,24,27</sup> However, the difference in the extent of thiolate desorption from the reduced Au38 cluster simply by changing the dispersing solvent from CB to DCE is quite unanticipated. From Figure 3c and d, it is clear that the extent of monolayer desorption for  $z = -2$  is far greater in DCE relative to that in CB as the detector current response is greater by a factor of  $\sim 5$ . The exact identity of the thiolate species desorbed is unknown and cannot be determined based on the simple experiments described here. It is, however, very unlikely to a simple thiolate based on recent understanding of the composition of the thiolate monolayer in gold clusters.<sup>3,10,11</sup>

**Cluster Stability in Excess Thiol Solution:** As the general synthesis procedure for isolating monodisperse Au38 is based on its stability in excess thiol relative to other core sizes,<sup>18,21</sup> we next considered the role of the solvent in this annealing process. Samples of as-synthesized particles were annealed in an excess thiol solution in both DCE and CB, and the resulting dispersity in core sizes was then compared using Pt microelectrode voltammetry. The SWV of the as-prepared



clusters given in Figure 4 (lower trace in both plots) is typical for polydisperse particles containing fractions of Au38 and larger clusters such as Au144. The charging peaks for the differing core sizes overlap, giving a composite SWV with peaks that vary in peak current and the voltage spacing between the peaks. As can be seen from the upper trace in Figure 4a, using DCE as the annealing solvent effectively removes the larger clusters, yielding highly monodisperse Au38. However, annealing in CB has a clearly different outcome. In this case, as can be seen in Figure 4b (upper trace), polydispersity increased with charging patterns, ascribable to at least two size fractions, Au38 and Au144, now clearly present in the voltammetric response.<sup>21,28</sup> From these experiments, it can be concluded that all other clusters except Au38 are etched in the presence of excess thiol in a DCE solution. By simply changing the solvent to CB, keeping all other parameters identical, Au38, Au144, and possibly other core sizes are stable in the presence of excess thiol. In neat thiol, Tsukuda and co-workers reported that both Au38 and Au144 are resistant to etching,<sup>7</sup> and our findings in the presence of excess thiol CB solution are consistent with this. However, our data show that a given cluster's ability to withstand thiol etching is dependent on the dispersing solvent. This unanticipated solvent dependence may explain the disparity between the reports in the literature on the effectiveness of annealing to improve dispersity.<sup>19–21,28–31</sup> In this case, it is surprising that the Au38 degrades with time in DCE solution but is stable indefinitely when excess thiol is added to solution. Additional theoretical insight is required to understand the underlying mechanism of this experimental observation.

The experimental results presented here point to a strong role of the solvent in the stability of MPCs. The origin of the effect may be in the organometallic nature of the protecting monolayer and its coordination with the solvent. This study is relevant for increasing the fundamental understanding of the properties of the Au thiolates protecting the core but is also more of practical relevance. From using MPCs as building blocks for nanoparticle superstructures to basic characterization studies, the solvent plays a critical role in their synthesis, purification, isolation, self-assembly, charging, surface functionalization, handling, shelf life, and so forth,<sup>6,32,33</sup> and as such, the influence of the solvent cannot be overlooked.

## EXPERIMENTAL DETAILS

Hexanethiolate-protected Au38 clusters were synthesized as previously reported.<sup>21</sup> The monodispersity was verified by electrochemical experiments and mass spectrometry (Supporting Information).<sup>21,34</sup> The data were consistent with clusters having the molecular formula Au<sub>38</sub>(SR)<sub>24</sub>.<sup>5,35</sup> The stability of the clusters in different dispersing solvents was studied using a combination of electrochemical measurements at both a Pt microelectrode–solution interface and at the micropipet supported water–organic interface. The former provides information on the concentration of a given redox species, here Au38, in the organic solution. The latter detects the presence of relatively hydrophilic ionic species in the organic phase as their transfer across the water–organic interface is detected as current in voltammetric experiments. The interfacial potential

difference ( $\Delta_0^w\phi$ ) at which a given ion transfers from one phase to the other is a measure of its lipophilicity. Cyclic voltammetric (CV) and square wave voltammetric (SWV) measurements were performed using a CHI 900 potentiostat (CH Instruments, Austin, TX). The same instrument in bipotentiostatic mode was used to control the interfacial potential difference ( $\Delta_0^w\phi$ ) applied to the liquid–liquid interface supported at the tip of the micropipet and to the platinum coat electrode (a schematic is given in Figure 3a). The SWV measurement parameters were as follows: increment  $E = 0.004$  V; amplitude = 0.025 V; frequency = 15 Hz; CV scan rates:  $0.1 \text{ V s}^{-1}$  for Pt coat measurements and  $0.05 \text{ V s}^{-1}$  for water/organic interface measurements. For the microelectrode CV and SWV measurements, a  $25 \mu\text{m}$  diameter Pt microelectrode was used as the working electrode and a silver wire as both counter and quasi-reference electrode (QRE). The particles were dispersed in DCE or CB solution with 10 mM bis(triphenylphosphoranylidene) ammonium tetrakis(pentafluorophenyl) borate (BisTPPATP-BF<sub>20</sub>) as the supporting electrolyte. O<sub>2</sub> was removed from solution by bubbling with N<sub>2</sub> prior to recording the voltammograms. For the micropipet-supported water–organic interface studies, platinum-coated micropipets with an inner diameter of  $25 \mu\text{m}$  were prepared as previously reported.<sup>23,24</sup> The platinum coat electrode acted as the first working electrode (WE1), with platinum (CE) and silver wires (RE1) in the organic phase serving as common organic counter and quasi-reference electrodes. The pipet was filled with an aqueous solution of 10 mM LiCl, and the water–organic interface formed at the tip was the second working electrode. The organic phase was identical to those used for the microelectrode voltammetric measurements. The applied interfacial potential was controlled using a silver wire dipped into the pipet as the aqueous quasi-reference electrode (QRE) (RE2 in the schematic in Figure 3a), with silver and platinum wires immersed in the organic phase serving as the organic-phase QRE and CE electrodes, respectively (RE1 and CE, respectively, in the schematic given in Figure 3a). For the simple voltammetric experiments at the liquid–liquid interface, the Pt coat electrode was not connected, while for the generation–collection mode experiments, it functioned as the generator electrode.

**ACKNOWLEDGMENT** Financial support from the Academy of Finland is gratefully acknowledged (B.M.Q. and O.T.). We are grateful to Thomas Krick (UM) for his assistance with MALDI-TOF measurements.

**SUPPORTING INFORMATION AVAILABLE** Additional details on synthesis, experimental arrangements for the microelectrode and micropipet experiments, and mass spectrometry characterization (LDI- and MALDI-TOF mass spectrometry). This material is available free of charge via the Internet at <http://pubs.acs.org>.

## AUTHOR INFORMATION

### Corresponding Author:

\* To whom correspondence should be addressed. E-mail: [bquinn@iki.fi](mailto:bquinn@iki.fi).

## REFERENCES

- (1) Wu, Z.; Gayathri, C.; Gil, R. R.; Jin, R. Probing the Structure and Charge State of Glutathione-Capped Au<sub>25</sub>(SG)<sub>18</sub> Clusters by NMR and Mass Spectrometry. *J. Am. Chem. Soc.* **2009**, *131*, 6535–6542.
- (2) Zhu, M.; Lanni, E.; Garg, N.; Bier, M. E.; Jin, R. Kinetically Controlled, High-Yield Synthesis of Au<sub>25</sub> Clusters. *J. Am. Chem. Soc.* **2008**, *130*, 1138–1139.
- (3) Zhu, M.; Aikens, C. M.; Hollander, F. J.; Schatz, G. C.; Jin, R. Correlating the Crystal Structure of A Thiol-Protected Au<sub>25</sub> Cluster and Optical Properties. *J. Am. Chem. Soc.* **2008**, *130*, 5883–5885.
- (4) Walter, M.; Akola, J.; Lopez-Acevedo, O.; Jadzinsky, P. D.; Calero, G.; Ackerson, C. J.; Whetten, R. L.; Grönbeck, H.; Häkkinen, H. A Unified View of Ligand-Protected Gold Clusters As Superatom Complexes. *Proc. Natl. Acad. Sci. U.S.A.* **2008**, *105*, 9157–9162.
- (5) Pei, Y.; Gao, Y.; Zeng, X. C. Structural Prediction of Thiolate-Protected Au<sub>38</sub>: A Face-Fused Bi-icosahedral Au Core. *J. Am. Chem. Soc.* **2008**, *130*, 7830–7832.
- (6) Murray, R. W. Nanoelectrochemistry: Metal Nanoparticles, Nanoelectrodes, and Nanopores. *Chem. Rev.* **2008**, *108*, 2688–2720.
- (7) Chaki, N. K.; Negishi, Y.; Tsunoyama, H.; Shichibu, Y.; Tsukuda, T. Ubiquitous 8 and 29 kDa Gold:Alkanethiolate Cluster Compounds: Mass-Spectrometric Determination of Molecular Formulas and Structural Implications. *J. Am. Chem. Soc.* **2008**, *130*, 8608–8610.
- (8) Tsunoyama, H.; Nickut, P.; Negishi, Y.; Al-Shamery, K.; Matsumoto, Y.; Tsukuda, T. Formation of Alkanethiolate-Protected Gold Clusters with Unprecedented Core Sizes in the Thiolation of Polymer-Stabilized Gold Clusters. *J. Phys. Chem. C* **2007**, *111*, 4153–4158.
- (9) Negishi, Y.; Chaki, N. K.; Shichibu, Y.; Whetten, R. L.; Tsukuda, T. Origin of Magic Stability of Thiolated Gold Clusters: A Case Study on Au<sub>25</sub>(SC<sub>6</sub>H<sub>13</sub>)<sub>18</sub>. *J. Am. Chem. Soc.* **2007**, *129*, 11322–11323.
- (10) Heaven, M. W.; Dass, A.; White, P. S.; Holt, K. M.; Murray, R. W. Crystal Structure of the Gold Nanoparticle [N(C<sub>8</sub>H<sub>17</sub>)<sub>4</sub>]-[Au<sub>25</sub>(SCH<sub>2</sub>CH<sub>2</sub>Ph)<sub>18</sub>]. *J. Am. Chem. Soc.* **2008**, *130*, 3754–3755.
- (11) Jadzinsky, P. D.; Calero, G.; Ackerson, C. J.; Bushnell, D. A.; Kornberg, R. D. Structure of a Thiol Monolayer-Protected Gold Nanoparticle at 1.1 Å. Resolution. *Science* **2007**, *318*, 430–433.
- (12) Häkkinen, H.; Walter, M.; Grönbeck, H. Divide and Protect: Capping Gold Nanoclusters with Molecular Gold-Thiolate Rings. *J. Phys. Chem. B* **2006**, *110*, 9927–31.
- (13) Shichibu, Y.; Negishi, Y.; Tsunoyama, H.; Kanehara, M.; Teranishi, T.; Tsukuda, T. Extremely High Stability of Glutathionate-Protected Au<sub>25</sub> Clusters against Core Etching. *Small* **2007**, *3*, 835–839.
- (14) Negishi, Y.; Takasugi, Y.; Sato, S.; Yao, H.; Kimura, K.; Tsukuda, T. Kinetic Stabilization of Growing Gold Clusters by Passivation with Thiolates. *J. Phys. Chem. B* **2006**, *110*, 12218–12221.
- (15) Negishi, Y.; Takasugi, Y.; Sato, S.; Yao, H.; Kimura, K.; Tsukuda, T. Magic-Numbered Au<sub>n</sub> Clusters Protected by Glutathione Monolayers ( $n = 18, 21, 25, 28, 32, 39$ ): Isolation and Spectroscopic Characterization. *J. Am. Chem. Soc.* **2004**, *126*, 6518–6519.
- (16) Schaaff, T. G.; Knight, G.; Shafigullin, M. N.; Borkman, R. F.; Whetten, R. L. Isolation and Selected Properties of a 10.4 kDa Gold:Glutathione Cluster Compound. *J. Phys. Chem. B* **1998**, *102*, 10643–10646.
- (17) Schaaff, T. G.; Shafigullin, M. N.; Khoury, J. T.; Vezmar, I.; Whetten, R. L.; Cullen, W. G.; First, P. N.; Wing, C.; Ascensio, J.; Yacaman, M. J. Isolation of Smaller Nanocrystal-Au Molecules: Robust Quantum Effects in Optical Spectra. *J. Phys. Chem. B* **1997**, *101*, 7885–7891.
- (18) Qian, H. F.; Zhu, M. Z.; Andersen, U. N.; Jin, R. C. Facile, Large-Scale Synthesis of Dodecanethiol-Stabilized Au-38 Clusters. *J. Phys. Chem. A* **2009**, *113*, 4281–4284.
- (19) Hicks, J. F.; Miles, D. T.; Murray, R. W. Quantized Double-Layer Charging of Highly Monodisperse Metal Nanoparticles. *J. Am. Chem. Soc.* **2002**, *124*, 13322–13328.
- (20) Jimenez, V. L.; Georganopoulou, D. G.; White, R. J.; Harper, A. S.; Mills, A. J.; Lee, D.; Murray, R. W. Hexanethiolate Monolayer Protected 38 Gold Atom Cluster. *Langmuir* **2004**, *20*, 6864–6870.
- (21) Toikkanen, O.; Ruiz, V.; Rönholm, G.; Kalkkinen, N.; Liljeroth, P.; Quinn, B. M. Synthesis and Stability of Monolayer-Protected Au<sub>38</sub> Clusters. *J. Am. Chem. Soc.* **2008**, *130*, 11049–11055.
- (22) Kim, J.; Lema, K.; Ukaigwe, M.; Lee, D. Facile Preparative Route to Alkanethiolate-Coated Au<sub>38</sub> Nanoparticles: Post-synthesis Core Size Evolution. *Langmuir* **2007**, *23*, 7853–7858.
- (23) Liljeroth, P.; Quinn, B. M.; Kontturi, K. Lipophilicity of Ions Electrogenated at a Pt Coated Micropipette Supported Liquid–Liquid Interface. *Electrochem. Commun.* **2002**, *4*, 255–259.
- (24) Quinn, B. M.; Kontturi, K. Reductive Desorption of Thiolate from Monolayer Protected Gold Clusters. *J. Am. Chem. Soc.* **2004**, *126*, 7168–7169.
- (25) Volkov, A. G.; Deamer, D. W. *Liquid–Liquid Interfaces, Theory and Methods*; CRC Press: Boca Raton, FL, 1996; p 41.
- (26) Schaaff, T. G. Laser Desorption and Matrix-Assisted Laser Desorption/Ionization Mass Spectrometry of 29-kDa Au:SR Cluster Compounds. *Anal. Chem.* **2004**, *76*, 6187–6196.
- (27) Antonello, S.; Holm, A. H.; Instuli, E.; Maran, F. Molecular Electron-Transfer Properties of Au<sub>38</sub> Clusters. *J. Am. Chem. Soc.* **2007**, *129*, 9836–9837.
- (28) Quinn, B. M.; Liljeroth, P.; Ruiz, V.; Laaksonen, T.; Kontturi, K. Electrochemical Resolution of 15 Oxidation States for Monolayer Protected Gold Nanoparticles. *J. Am. Chem. Soc.* **2003**, *125*, 6644–6645.
- (29) Miles, D. T.; Murray, R. W. Temperature-Dependent Quantized Double Layer Charging of Monolayer-Protected Gold Clusters. *Anal. Chem.* **2003**, *75*, 1251–1257.
- (30) Wu, Z.; Suhan, J.; Jin, R. C. One-Pot Synthesis of Atomically Monodisperse, Thiol-Functionalized Au-25 Nanoclusters. *J. Mater. Chem.* **2009**, *19*, 622–626.
- (31) Donkers, R. L.; Lee, D.; Murray, R. W. Synthesis and Isolation of the Molecule-like Cluster Au<sub>38</sub>(PhCH<sub>2</sub>CH<sub>2</sub>S)<sub>24</sub>. *Langmuir* **2004**, *20*, 1945–1952.
- (32) Daniel, M.-C.; Astruc, D. Gold Nanoparticles: Assembly, Supramolecular Chemistry, Quantum-Size-Related Properties, and Applications toward Biology, Catalysis, and Nanotechnology. *Chem. Rev.* **2004**, *104*, 293–346.
- (33) Love, J. C.; Estroff, L. A.; Kriebel, J. K.; Nuzzo, R. G.; Whitesides, G. M. Self-Assembled Monolayers of Thiolates on Metals as a Form of Nanotechnology. *Chem. Rev.* **2005**, *105*, 1103–1169.
- (34) Dass, A.; Stevenson, A.; Dubay, G. R.; Tracy, J. B.; Murray, R. W. Nanoparticle MALDI-TOF Mass Spectrometry without

Fragmentation: Au<sub>25</sub>(SCH<sub>2</sub>CH<sub>2</sub>Ph)<sub>18</sub> and Mixed Monolayer Au<sub>25</sub>(SCH<sub>2</sub>CH<sub>2</sub>Ph)<sub>18-x</sub>(L)<sub>x</sub>. *J. Am. Chem. Soc.* **2008**, *130*, 5940–5946.

- (35) Jiang, D.-e.; Luo, W.; Tiago, M. L.; Dai, S. In Search of a Structural Model for a Thiolate-Protected Au<sub>38</sub> Cluster. *J. Phys. Chem. C* **2008**, *112*, 13905–13910.